

Dynamic M -Shell Effects in the Ultraviolet Absorption Spectrum of Metallic Potassium

A. C. Tselis and A. W. Overhauser

Department of Physics, Purdue University, West Lafayette, Indiana 47907

(Received 20 November 1984)

The filled M shell of potassium, set into oscillation by the electric field of a photon, leads to interband transitions that explain a large absorption peak at 8 eV. Interference between this collective perturbation and the ordinary $\mathbf{A} \cdot \mathbf{p}$ coupling (between a photon and conduction electron) shows that the sign of the V_{110} pseudopotential is negative.

PACS numbers: 78.20.-e, 32.30.Jc, 32.80.-t, 78.65.Ez

Twelve years ago Whang, Arakawa, and Callcott¹ discovered a large ultraviolet absorption near 8 eV in metallic potassium. Their data are shown in Fig. 1, which includes the Drude absorption (below 1 eV) and the Wilson-Butcher interband peak at 2 eV. Explanation of the ultraviolet peak, which also occurs in Rb and Cs,¹ has remained elusive. Hermanson² showed that it could not be attributed to plasmons; and an attempt³ with a limited-basis-set, tight-binding model for the conduction band (instead of a nearly free-electron one) led only to a weak and highly structured absorption.

We show here that the absorption in K near 8 eV arises from a collective contribution to the ordinary interband matrix element. It is caused by the interaction of a conduction electron with the dynamic oscillation of the eight M -shell electrons. A nearly free-electron, pseudopotential approximation is the method we employ.

The periodic pseudopotential acting on a conduction electron can be divided into two parts:

$$V(\mathbf{r}) = V_M(\mathbf{r}) + V_I(\mathbf{r}). \quad (1)$$

V_I is the inner ion-core potential, caused by the nuclei

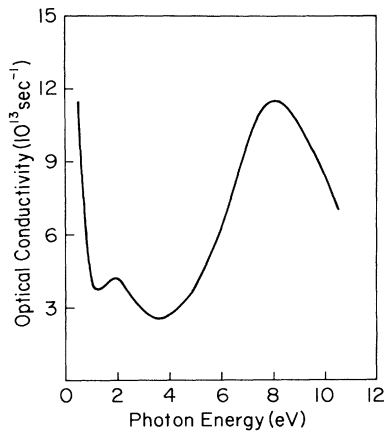


FIG. 1. Experimental, room-temperature, absorption spectrum of potassium. The rise below 1 eV is the Drude absorption. The Wilson-Butcher interband peak is at 2 eV. Data are from Ref. 1.

and their ten tightly bound K - and L -shell electrons. We shall take V_I to be the Coulomb potential of a static bcc array of point ions, each having charge $9e$. V_M is the pseudopotential of the M shells. In the electric field of a photon, described by a vector potential $A \hat{\mathbf{x}} \cos \omega t$, the eight M -shell electrons (on each ion) undergo a coherent oscillation of amplitude a . Accordingly, the static V_M must be replaced by a dynamic one:

$$V_M(\mathbf{r}) \rightarrow V_M(\mathbf{r} - a \hat{\mathbf{x}} \sin \omega t). \quad (2)$$

The shell model of Dick and Overhauser⁴ can be used (with Newton's second law) to calculate the amplitude of the oscillation, $x = a \sin \omega t$:

$$8m\ddot{x} = -8m\omega_M^2 x - (8e\omega/c)A \sin \omega t. \quad (3)$$

$8m\omega_M^2$ is the shell-model spring constant; its value will be discussed below. The amplitude which satisfies Eq. (3) is

$$a = \omega e A / mc (\omega^2 - \omega_M^2). \quad (4)$$

The shell model should be applicable as long as ω is small compared to ω_M .

In the nearly free-electron model, optical absorption is attributed to transitions (in the extended-zone scheme) from \mathbf{k} to $\mathbf{k} + \mathbf{G}$, as shown in Fig. 2. Consider one of the $[110]$ reciprocal-lattice vectors, \mathbf{G} , and take it to be along $\hat{\mathbf{x}}$. The initial-state wave function, corrected to first order in the pseudopotential, is

$$\psi_{\mathbf{k}} \cong e^{i\mathbf{k} \cdot \mathbf{r}} - [V_{110}/W(\mathbf{k})] e^{i(\mathbf{k} + \mathbf{G}) \cdot \mathbf{r}}, \quad (5)$$

where V_{110} is the \mathbf{G} Fourier coefficient of $V(\mathbf{r})$, Eq. (1). $W(\mathbf{k})$ is the transition energy:

$$W(\mathbf{k}) = E(\mathbf{k} + \mathbf{G}) - E(\mathbf{k}). \quad (6)$$

The final-state wave function is

$$\psi_{\mathbf{k} + \mathbf{G}} \cong e^{i(\mathbf{k} + \mathbf{G}) \cdot \mathbf{r}} + [V_{110}/W(\mathbf{k})] e^{i\mathbf{k} \cdot \mathbf{r}}. \quad (7)$$

The time-dependent perturbation which connects (5) to (7) arises from the $\mathbf{A} \cdot \mathbf{p}$ coupling with the photon and also from the oscillatory part, ΔV_M , of the M -shell potential (2), having Fourier periodicity \mathbf{G} :

$$\Delta V_M = V_{MG} e^{i\mathbf{G} \cdot \mathbf{r}} (-iaG \sin \omega t). \quad (8)$$

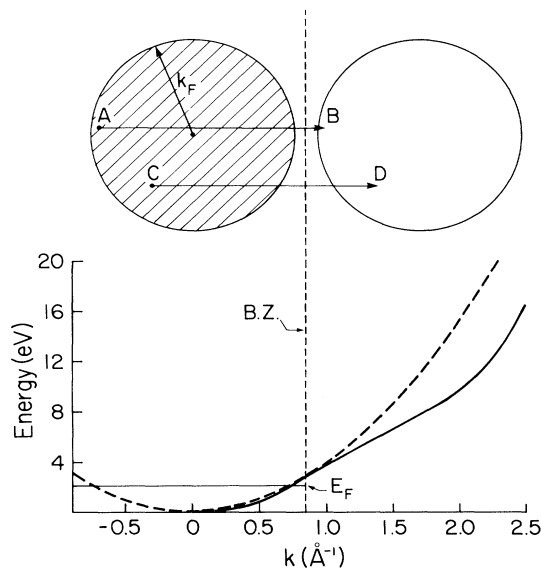


FIG. 2. Interband transitions from occupied states of the Fermi sphere to empty, excited states. The wave-vector change ($A \rightarrow B$ or $C \rightarrow D$) is \mathbf{G} , a [110] reciprocal-lattice vector. The solid curve is the electronic $E(k)$ given by Eq. (18); the dashed curve is a free-electron parabola. A Brillouin-zone boundary is shown.

This expression is the leading term in an expansion of $\exp[i\mathbf{G} \cdot (\mathbf{r} - a\hat{\mathbf{x}}\sin\omega t)]$ in powers of a . Higher Fourier components of V_M affect absorption only above 20 eV. Optical transitions arise from (the positive-frequency part of) the total perturbation,

$$H' = (eA/mc)p_x \cos\omega t - iaGV_{MG} e^{i\mathbf{G} \cdot \mathbf{r}} \sin\omega t. \quad (9)$$

The first term is the only one that is usually considered. Collective effects, analogous to the second term, have been discussed for atomic transitions,⁵ in a time-dependent Hartree-Fock formalism, and usually lead to only small corrections.

For alkali metals, the first term of (9), which causes the Wilson-Butcher interband peak,⁶ is small because p_x connects the large term of (5) with the small term of (7), and vice versa. Because of the factor $\exp(i\mathbf{G} \cdot \mathbf{r})$, the M -shell term of H' connects the large terms of both (5) and (7). That is one reason why the M -shell effect is relatively more important here. The (positive-frequency) matrix element of H' between initial and final states is

$$\langle \mathbf{k} + \mathbf{G} | H' | \mathbf{k} \rangle = \frac{-e\hbar GA}{2mcW} \left[V_{110} + \frac{W^2}{(\hbar\omega_M)^2 - W^2} V_{MG} \right], \quad (10)$$

when we have used Eq. (4) and $W = \hbar\omega$ is the transition energy. Note that both terms (in square brackets) are real, so that there will be an interference

phenomenon between the two contributions. This effect will permit an experimental determination of the sign of V_{110} , the potential which causes energy gaps at the Brillouin-zone boundary.

We now turn to a discussion of the Fourier coefficients, V_{110} and V_{MG} . The Fourier-transform version of Eq. (1) for the [110] reciprocal-lattice vector \mathbf{G} is

$$V_{110} = V_{MG} + V_{IG}. \quad (11)$$

The magnitude of V_{110} , estimated by an analysis of de Haas-van Alphen data,⁷ is

$$V_{110} \approx -0.2 \text{ eV}. \quad (12)$$

We have inserted the negative sign as a consequence of our conclusion below. Since \mathbf{G} is here the smallest reciprocal-lattice vector, we may take the inner-ion-core term (charge = $9e$) to be (Ω is the atomic volume)

$$V_{IG} \approx -36\pi e^2 / \Omega G^2 = -7.9 \text{ eV}, \quad (13)$$

since the form factor of the ten inner-core electrons is ≈ 10 for wave vector \mathbf{G} . It follows from Eqs. (11) to (13) that

$$V_{MG} \approx 7.7 \text{ eV}. \quad (14)$$

Note that V_{MG} is 40 times larger than V_{110} . From Eq. (10) it is easy to understand why the oscillator strength of the M -shell-mediated peak is 2 orders of magnitude larger than the Wilson-Butcher one.

The only parameter of Eq. (10) that remains to be determined is ω_M which, from Eq. (3), is the resonant frequency of the M -shell oscillation. For a free K^+ ion, the shell-model spring constant⁴ can be found by fitting the K^+ polarizability,⁸ $\alpha = 0.9 \times 10^{-24} \text{ cm}^2$. This approach leads to a free-ion, M -shell resonance at $\hbar\omega = 31 \text{ eV}$. However, in the metal, this resonance will be shifted to a smaller frequency as a result of interaction of each M shell with the ionic potentials of near neighbors. (There is also a small reduction from the dielectric screening of the conduction electrons.) A theoretical estimate of the shift is $\sim -7 \text{ eV}$.⁹ However, it is not necessary to depend on such calculations, since the M -shell resonant frequency has been measured for K by synchrotron-radiation absorption¹⁰ and is

$$\hbar\omega_M \approx 26 \text{ eV}. \quad (15)$$

We emphasize here that all of the parameters appearing in the interband matrix element, Eq. (10), are determined from independent experiments. (The vector potential A , of course, disappears when the optical absorption is evaluated.)

The optical conductivity σ can be computed if we equate the mean "Joule heating" to the golden-rule transition-rate times W , i.e.,

$$\frac{1}{2} \sigma E^2 = 8W [(2\pi/\hbar) \langle \mathbf{k} + \mathbf{G} | H' | \mathbf{k} \rangle^2 \rho(W)], \quad (16)$$

where E is the peak electric field ($\omega A/c$) and $\rho(W)$ is the joint density of states (per spin). The factor 8 includes a factor 2 for spin and a factor, $12(\cos^2\theta)_{\text{av}} = 4$, to account for the twelve $[110]$ \mathbf{G} 's and their average polarization factor. (θ is the angle between $\hat{\mathbf{x}}$ and \mathbf{G} .) Accordingly, the optical conductivity is

$$\sigma = \frac{8\pi e^2 \hbar^3 G^2}{m^2 W^3} \left[V_{110} + \frac{W^2}{(\hbar\omega_M)^2 - W^2} V_{MG} \right]^2 \rho(W). \quad (17)$$

This result reduces to Butcher's formula⁶ if the M shells are rigidly bound ($\omega_M = \infty$), and if $\rho(W)$ is calculated from Eq. (16) with $E = \hbar^2 k^2/2m$.

Band calculations¹¹ show that $E(k)$ is not free-electron-like beyond the (first) Brillouin zone. Therefore we use an $E(k)$ which behaves appropriately beyond $k = G/2$. We accomplish this with the following heuristic function:

$$E = \frac{\hbar^2 k^2}{2m} \frac{1 + 0.08u^4}{1 + 0.55u^2}, \quad (18)$$

where $u = (2k/G) - 1$. The u^2 in the denominator provides a "sag" which allows $E(k)$ to "fit" the band calculations in the second zone. The u^4 in the numerator enables $E(k)$ to resume its parabolic course for larger k . The function given by Eq. (18) is shown in Fig. 2. The sag at $k = G$, relative to the free-electron parabola (also shown), is ~ 4 eV. Such a value is consistent with the band structure.

Since $E(k)$, given by Eq. (18), cannot be factored into x , y , and z components, $\rho(\omega)$ must be calculated numerically. The resulting $\sigma(\omega)$ is shown in Fig. 3. The observed Drude absorption has been added to Eq. (17) in order to facilitate comparison with the experimental spectrum of Fig. 1. The M -shell-mediated absorption (taken alone) is the curve having $V_{110} = 0$. Comparison of the other two curves, with $V_{110} = \pm 0.2$ eV, shows the extraordinary interference effect between the $\mathbf{A} \cdot \mathbf{p}$ interaction and the dynamic M -shell potential. It is obvious that V_{110} must be negative. Most pseudopotential form factors, $V(q)$, found in the literature, though negative for small q , change sign and are positive at $q = G$. One notable exception is the nonlocal potential of Rasolt and Taylor,¹² which remains negative.

The small value of σ near 4 eV (for the solid curve of Fig. 3) is caused by exact cancellation of the two terms in the matrix element (10). Only the Drude tail contributes at 4 eV. This is an artifact caused by our neglect of damping. The conduction electrons (undergoing interband transitions) will exert a reaction force. A small phase shift relative to the M -shell oscillation will then prevent the interference dip near 4 eV from being so dramatic.⁹

The remarkable agreement in the height and width

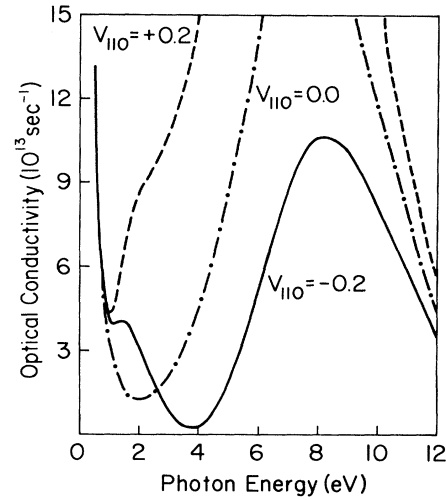


FIG. 3. Theoretical optical-absorption spectrum of potassium computed from Eq. (17), for three values of the pseudopotential V_{110} . The experimental Drude absorption has been added. The peak at 8 eV is caused by the M -shell-mediated photon-electron interaction.

of the 8-eV peak leaves little doubt that the dynamic M -shell mechanism is responsible. The only adjusted parameters were those in Eq. (18), which affect somewhat the energy of the ultraviolet peak. It seems likely that dynamic polarization will be important in the vacuum-ultraviolet spectra of other materials.

The authors are grateful to the National Science Foundation for support of this research.

¹U. S. Whang, E. T. Arakawa, and T. A. Callcott, Phys. Rev. B **6**, 2109 (1972).

²J. Hermanson, Phys. Rev. B **6**, 400 (1972).

³W. Y. Ching and J. Callaway, Phys. Rev. Lett. **30**, 441 (1973).

⁴B. G. Dick, Jr. and A. W. Overhauser, Phys. Rev. **112**, 90 (1958).

⁵A. Dalgarno and G. A. Victor, Proc. Roy. Soc. London, Ser. A **291**, 291 (1966).

⁶P. N. Butcher, Proc. Phys. Soc. London, Sect. A **64**, 765 (1951).

⁷N. Ashcroft, Phys. Rev. **140**, A935 (1965). A similar analysis [M. J. G. Lee, in *Computational Methods in Band Theory*, edited by P. M. Marcus, J. F. Janak, and A. R. Williams (Plenum, New York, 1971)] leads to $|V_{110}| \sim 0.07$ eV, a value which underestimates the Wilson-Butcher peak by an order of magnitude.

⁸A. Dalgarno, Adv. Phys. **11**, 281 (1962).

⁹A. C. Tselis and A. W. Overhauser, unpublished.

¹⁰S. Sato, T. Miyahara, T. Hanyu, S. Yamaguchi, and T. Ishii, J. Phys. Soc. Jpn. **47**, 836 (1979).

¹¹F. S. Ham, Phys. Rev. **128**, 82 (1962).

¹²M. Rasolt and R. Taylor, Phys. Rev. B **11**, 2717 (1975).